New Mechanism for Fluxionality in Triiron Carbonyl Clusters. Syntheses, Crystal Structure Determination, and Variable-Temperature ^{13}C NMR Study of Trifluoromethyl Isocyanide Substituted Derivatives of Dodecacarbonyltriiron

Dieter Lentz* and Robert Marschall

Institut für Anorganische und Analytische Chemie der Freien Universität Berlin, Fabeckstrasse 34-36, D-1000 Berlin 33, FRG

Received August 21, 1990

The trifluoromethyl isocyanide substituted derivatives of dodecacarbonyltriiron $Fe_3(CO)_{10}(L)(CNCF_3)$ **4a–e** (L = $P(CH_3)_3$ (**a**), $P(C_2H_5)_3$ (**b**), $P(OCH_3)_3$ (**c**), $P(OC_2H_5)_3$ (**d**), and CN-*t*-C_4H_9 (**e**)) were synthesized from $Fe_3(CO)_{11}(L)$ by using trimethylamine *N*-oxide to generate the labile acetonitrile complex $Fe_3(CO)_{10}(L)(CH_3CN)$, which undergoes ligand exchange with trifluoromethyl isocyanide. According to the NMR spectra, **4a** and **4b** exist as single isomers, whereas for **4c,d** and **4e** two and three isomers could be detected. The activation barriers for the isomerization of **4(I)c,d** and **4(II)c,d** were determined by variable-temperature NMR spectroscopy. The structures of **4a**, **4(I)c**, and **4(II)c** were determined by X-ray crystal structure analysis: **4a**, orthorhombic, *Pbca*, a = 1529.4 (12) pm, b = 1585.2 (9) pm, c = 1887.7 (12) pm; **4(I)c**, orthorhombic, *Pbca*, a = 1552.0 (4) pm, b = 1619.9 (5) pm, c = 1962.6 (4) pm; **4(II)c**, triclinic, $P\bar{1}$, a = 840.0 (3) pm, 1173.4 (6) pm, 1337.4 (6) pm, α = 69.42 (3)°, β = 90.37 (3)°, γ = 75.65 (3)°. In all of these compounds the trifluoromethyl isocyanide ligand occupies a bridging position, both in the solid state and in solution. According to the crystal structure analysis, the phosphine and phosphite ligand are bonded in an equatorial position at the bridged iron atom for compounds **4a** and **4(I)c** or unbridged iron atom from compound **4(II)c**, respectively. All of these compounds **4a–d** are nonrigid on the NMR time scale at ambient temperature. In contrast to $Fe_3(CO)_{12}$ and its phosphine- and phosphite-substituted derivatives, the scrambling of the carbonyl ligands can be slowed down at −80 °C, so that all of the resonances expected from the solid-state structure can be observed in the ^{13}C NMR spectra. With the aid of the phosphorus–carbon coupling an unambiguous assignment of the signals can be made. This allows a reassignment of the spectrum of $Fe_3(CO)_{11}(CNCF_3)$. From the experimental data a uniform ligand exchange mechanism could be developed for all of these compounds.

Introduction

The solid-state structure of dodecacarbonyltriiron is unambiguously established since Dahl et al. carried out a X-ray crystal structure determination.[1] MAS ^{13}C NMR studies[2] have shown that a fluxional process occurs even in solid $Fe_3(CO)_{12}$. These data have been rationalized by two different processes. Dorn and Hanson explained their results in terms of a rotation of the iron triangle around a 3-fold axis perpendicular to the iron triangle.[2] Johnson et al. stated that such a process is unlikely in respect of the thermal ellipsoids of the iron atoms.[3] They proposed that the MAS ^{13}C NMR spectra can as well be rationalized by small rotation of the iron triangle around the pseudo 2-fold axis through the unbridged iron atom perpendicular to the iron–iron edge.

The structure of $Fe_3(CO)_{12}$ in solution is still under discussion. Various IR experiments[4–8] have been interpreted in terms of either a bridged structure, as found in the X-ray structure determination in the solid state, or in terms of a nonbridged structure similar to that found for $Ru_3(CO)_{12}$[9] and $Os_3(CO)_{12}$.[10] The infrared spectrum of $Fe_3(CO)_{12}$ in an argon matrix at 20 K is consistent with the bridged solid-state structure.[11] It was concluded from a recent IR study of $Fe_3(CO)_{12}$ in solution that the compound exists as a mixture of bridged and unbridged species.[12]

According to variable-temperature ^{13}C NMR studies[13,14] $Fe_3(CO)_{12}$ in solution is a highly fluxional molecule with the carbonyl groups being equivalent on the NMR time scale even at −150 °C. This very low energy process ($\Delta G^{\ddagger} < 6$ kcal/mol) has been explained by Cotton and Troup by a "merry-go-round" mechanism[14] which requires simultaneous opening and closing of the carbonyl bridges. An alternative mechanism proposed by B. F. G. Johnson et al. consists of a rotation of the iron triangle around the pseudo 2-fold axis resulting in a nonbridged pseudo D_3 structure.[15] Further rotation generates a structure with triply bridging carbonyl ligands. Recent EXAFS studies[16] of $Fe_3(CO)_{12}$ in frozen solutions revealed that in hexane $Fe_3(CO)_{12}$ most likely possesses the nonbridged D_3 structure, whereas frozen solutions in the more polar dichloromethane contain both bridged and nonbridged species.

Various phosphine and phosphite derivatives of $Fe_3(CO)_{12}$ have been synthesized in order to increase the activation barrier of the ligand exchange process. Johnson et

(1) Wei, C. H.; Dahl, L. F. *J. Am. Chem. Soc.* **1966**, *88*, 1821.
(2) Dorn, H.; Hanson, B. E.; Motell, E. *Inorg. Chim. Acta* **1981**, *54*, L71. Hanson, B. E.; Lisic, E. C.; Petty, J. T.; Iannaconne, G. A. *Inorg. Chem.* **1986**, *25*, 4062.
(3) Anson, C. E.; Benfield, R. E.; Bott, A. W.; Johnson, B. F. G.; Braga, D.; Marseglia, E. A. *J. Chem. Soc., Chem. Commun.* **1988**, 898.
(4) Sheline, R. K. *J. Am. Chem. Soc.* **1951**, *73*, 1615.
(5) Cable, J. W.; Sheline, R. K. *Chem. Rev.* **1965**, *56*, 1.
(6) Wilkinson, G.; Cotton, F. A. *J. Am. Chem. Soc.* **1957**, *79*, 752.
(7) Noack, K. *Helv. Chim. Acta* **1962**, *4*, 1847.
(8) Dobson, G. R.; Sheline, R. K. *Inorg. Chem.* **1963**, *2*, 1313.
(9) Churchill, M. R.; Hollander, F. J.; Hutchinson, J. P. *Inorg. Chem.* **1977**, *16*, 2655.
(10) Dahl, L. F., Corey, E. R. *Inorg. Chem.* **1962**, *1*, 521.
(11) Poliakoff, M.; Turner, J. J. *J. Chem. Soc., Chem. Comm.* **1970**, 1008.
(12) Dobbs, S.; Nunziante-Cesaro, S.; Maltese, M. *Inorg. Chim. Acta* **1986**, *113*, 167.
(13) Cotton, F. A.; Hunter, D. L. *Inorg. Chim. Acta* **1974**, *11*, L9.
(14) Cotton, F. A.; Troup, J. M. *J. Am. Chem. Soc.* **1974**, *96*, 4155.
(15) Johnson, B. F. G. *J. Chem. Soc., Chem. Comm.* **1976**, 703.
(16) Binstedt, N.; Evans, J.; Greaves, N.; Price, R. J. *J. Chem. Soc., Chem. Comm.* **1987**, 1330.

0276-7333/91/2310-1487$02.50/0

al.[17a] have developed a complicated process involving a rearrangement of the distorted icosohedral ligand polyhedron via a cuboctahedral polyhedron to explain their variable-temperature ^{13}C NMR results. As has been shown recently by Mann et al. the variable-temperature ^{13}C NMR spectra of $Fe_3(CO)_{11}(L)$, $Fe_3(CO)_{10}(L)_2$, and $Fe_3(CO)_9(L)_3$ can be well explained by a "merry-go-round mechanism".[18] In none of these compounds could be low-temperature limiting spectra which correspond to a rigid structure be obtained. Recently Johnson et al.[17b] developed a general mechanism for dynamic processes of trinuclear carbonyl clusters $M_3(CO)_{12}$ (M = Fe, Ru, or Os) and their derivatives with terminal-coordinated ligands based on the ligand polyhedral model.

We have recently synthesized undecacarbonyl(trifluoromethyl isocyanide)triiron.[19] According to the crystal structure determination the isocyanide ligand and one carbonyl ligand occupy the bridging positions in the solid state.[19] As the infrared spectra of solid $Fe_3(CO)_{11}(CNCF_3)$ and dissolved $Fe_3(CO)_{11}(CNCF_3)$ both show absorptions for a bridging carbonyl and a bridging trifluoromethyl isocyanide ligand, one can conclude that $Fe_3(CO)_{11}(CNCF_3)$ has similar structures in solution and the solid state.[19] The ^{13}C NMR spectrum of $Fe_3(CO)_{11}(CNCF_3)$ at −100 °C exhibits all of the signals which are expected on the basis of the solid-state structure.[20] On warming, a fluxional process starts above −80 °C but the signal of the isocyanide ligand does not show any change up to ambient temperature. Due to problems in the unambiguous assignment of the carbonyl resonances the proposed exchange mechanism has remained speculative.[20]

Herein we report the syntheses, X-ray structure determination, and variable-temperature NMR studies of the phosphine and phosphite derivatives $Fe_3(CO)_{10}(L)(CNCF_3)$.

Experimental Section

All reactions were carried out under dry argon by using standard Schlenk and vacuum techniques. Volatile materials were handled on a conventional glass vacuum line and amounts were determined by PVT techniques. ^1H, ^{19}F, ^{31}P, and ^{13}C NMR spectra were recorded by using a JEOL FX 90Q instrument with TMS, $CFCl_3$, H_3PO_4, and TMS or solvent signals as reference standards. Infrared spectra were taken on a Perkin-Elmer 883 instrument. Mass spectra were obtained on a Varian MAT 711 (80 eV). $Fe_3(CO)_{12}$,[21] $CNCF_3$,[22] $Fe_3(CO)_{11}[P(OCH_3)_3]$[23] (**1c**), and $Fe_3(CO)_{11}[P(OC_2H_5)_3]$[23] (**1d**) were prepared by literature methods. The compounds $Fe_3(CO)_{11}[P(CH_3)_3]$ (**1a**), $Fe_3(CO)_{11}[P(C_2H_5)_3]$ (**1b**), and $Fe_3(CO)_{11}(CN\text{-}t\text{-}C_4H_9)$ (**1e**) were prepared analogiously to **1c**. The physical and spectroscopic data of **1a,b**, and **e** were in accord with those reported.[24,25] Trimethylamine *N*-oxide (FLUKA) was sublimed in vacuum (95 °C/10^{-2} mbar) before use. The solvents dichloromethane (Merck p.A.) and acetonitrile (Merck p.A.) were saturated with argon. Samples for low-temperature NMR studies were prepared by adding CD_2Cl_2 to compounds **4a–d** in an NMR tube (5- or 10-mm diameter). After connecting to the vacuum line the sample was cooled to −78 °C and evacuated. SO_2ClF was condensed onto the sample. The tube was either sealed under vacuum or flushed with argon and closed.

General Procedure for the Preparation of the Clusters $Fe_3(CO)_{10}(\mu\text{-}CNCF_3)(L)$ (4a–e). Trimethylamine *N*-oxide (120 mg, 1.6 mmol) was added at −40 °C to a solution of **1a–e** (1.1–1.4 mmol) in 10 mL of acetonitrile and 250 mL of dichloromethane. The reaction mixture was allowed to warm to −5 °C within 2 h. The solution was cooled again to −40 °C, and the excess of trimethylamine *N*-oxide was removed by flash chromatography with silica (Woelm 63–200 μm, l = 5 cm, d = 1.5 cm). Trifluoromethyl isocyanide **3** (6 mmol) was condensed onto this olive-green solution at −196 °C by using the vacuum line system. The reaction mixture was stirred at −78 °C for 18 h. The solvent was removed in vacuum at −20 °C, and the residue was purified by column chromatography (silica, Woelm 63–200 μm, l = 15 cm, d = 5 cm, light petroleum 40–60 °C/dichloromethane 10:1). The first fraction was collected, pumped to dryness, and recrystallized from *n*-pentane.

4a: dark green crystals, yield 142 mg (21%), mp 126 °C. MS (80 eV): m/z 619 (M^+, 4), 563 (M − $2CO^+$, 20), 535 (M − $3CO^+$, 20), 507 (M − $4CO^+$, 5), 479 (M − $5CO^+$, 7), 451 (M − $6CO^+$, 23), 423 (M − $7CO^+$, 14), 395 (M − $8CO^+$, 7), 367 (M − $9CO^+$, 34), 339 (M − $10CO^+$, 100), and smaller fragment ions. $C_{15}H_9F_3Fe_3NO_{10}P$ (618.74) calcd C 29.12, H 1.47, N 2.26; found C 29.73, H 2.05, N 2.45. Molecular weight: calcd 618.7964, found 618.7969 (MS).

4b: dark green crystals, yield 595 mg (45%), mp 66 °C. MS (80 eV): m/z 661 (M^+, 1), 633 (M − CO^+, 0.3), 605 (M − $2CO^+$, 11), 577 (M − $3CO^+$, 18), 549 (M − $4CO^+$, 3), 521 (M − $5CO^+$, 6), 493 (M − $6CO^+$, 19), 465 (M − $7CO^+$, 8), 437 (M − $8CO^+$, 8), 409 (M − $9CO^+$, 27), 381 (M − $10CO^+$, 100), and smaller fragment ions. $C_{18}H_{15}F_3Fe_3NO_{10}P$ (660.82) calcd C 32.72, H 2.29, N 2.12; found C 33.35, H 2.95, N 2.14. Molecular weight: calcd 660.8434, found 660.8436 (MS).

4c: dark green crystals, yield 510 mg (55%), mp 86 °C. MS (80 eV): m/z 667 (M^+, 5), 639 (M − CO^+, 3), 611 (M − $2CO^+$, 25), 583 (M − $3CO^+$, 18), 555 (M − $4CO^+$, 21), 527 (M − $5CO^+$, 7), 499 (M − $6CO^+$, 8), 471 (M − $7CO^+$, 26), 443 (M − $8CO^+$, 42), 415 (M − $9CO^+$, 31), 387 (M − $10CO^+$, 100), and smaller fragment ions. $C_{15}H_9F_3Fe_3NO_{13}P$ (666.74) calcd C 27.02, H 1.36, N 2.11; found C 27.29, H 1.63, N 2.18. Molecular weight: calcd 666.7811; found 666.7815 (MS).

4d: dark green crystals, yield 460 mg (59%), mp 72 °C. MS (80 eV): m/z 653 (M − $2CO^+$, 4), 625 (M − $3CO^+$, 7), 597 (M − $4CO^+$, 11), 513 (M − $7CO^+$, 9), 485 (M − $8CO^+$, 23), 457 (M − $9CO^+$, 27), 429 (M − $10CO^+$, 100), and smaller fragment ions. $C_{18}H_{15}F_3Fe_3NO_{13}P$ (708.82) calcd C 30.50, H 2.13, N 1.98; found C 30.72, H 2.58, N 1.99.

4e: dark green crystals, yield 621 mg (71%), mp 93 °C. MS (80 eV): m/z 626 (M^+, 4), 598 (M − CO^+, 3), 570 (M − $2CO^+$, 19), 542 (M − $3CO^+$, 27), 514 (M − $4CO^+$, 7), 486 (M − $5CO^+$, 8), 458 (M − $6CO^+$, 37), 430 (M − $7CO^+$, 19), 402 (M − $8CO^+$, 9), 374 (M − $9CO^+$, 42), 346 (M − $10CO^+$, 100), and smaller fragment ions. $C_{17}H_9F_3Fe_3N_2O_{10}$ (625.80) calcd C 32.63, H 1.45, N 4.48; found C 32.35, H 2.34, N 4.41. Molecular weight: calcd 625.8257; found 625.8266 (MS).

Crystal Structure Analysis. The crystallographic data and intensity data collection of the compounds **4a**, **4(I)c**, and **4(II)c** are summarized in Table I. The data were collected by using a STOE diffractometer and reduced to structure factors by correction of Lorentz and polarization effects. A empirical absorption correction DIFABS[26] was applied. The structures were solved by Patterson methods, SHELXS-86.[27] Successive difference Fourier maps and least-squares refinement cycles, SHELX-76,[28] revealed the positions of all non-hydrogen atoms. To minimize the number of variables the CF_3 groups were refined as rigid groups C–F 132.4 pm, F–C–F 108.8°. SCHAKAL[29] and ORTEP[30] were used for molecular drawings. The final fractional coordinates of **4a**, **4(I)c**, and **4(II)d** are listed in Tables II–IV. Important bond

(17) (a) Benfield, R. E.; Gavens, P. D.; Johnson, B. F. G.; Mays, M. J.; Aime, S.; Milone, L.; Ostella, D. *J. Chem. Soc. Dalton Trans.* **1981**, 1535. (b) Johnson, B. F. G.; Bott, A. *J. Chem. Soc. Dalton Trans.* **1990**, 2437.
(18) Adams, H.; Bailey, N. A.; Bentley, G. W.; Mann, B. E. *J. Chem. Soc. Dalton Trans.* **1989**, 1831.
(19) Brüdgam, I.; Hartl, H.; Lentz, D. *Z. Naturforsch.* **1984**, *39b*, 721.
(20) Lentz, D. *Z. Naturforsch.* **1987**, *42b*, 839.
(21) *Handbuch der Präparativen Anorganischen Chemie*, 3rd ed.; G. Brauer, editor, Enke Verlag: Stuttgart, 1981; p 1828.
(22) Lentz, D. *J. Fluorine Chem.* **1984**, *24*, 523.
(23) Cardin, C. J.; Cardin, D. J.; Kelly, N. B.; Lawless, G. A.; Power, M. B. *J. Organomet. Chem.* **1988**, *341*, 447.
(24) Grant, S. M.; Manning, A. R. *Inorg. Chim. Acta* **1978**, *31*, 41.
(25) Bruce, M. I.; Hambley, T. W.; Nicholson, B. K. *J. Chem. Soc. Dalton Trans.* **1983**, 2385.
(26) Walker, N.; Stuart, D. *Acta Crystallogr., Sect. A* **1983**, *A39*, 158.
(27) Sheldrick, G. M. SHELXS-86 Program for Crystal Structure Solution, Göttingen, 1986.
(28) Sheldrick, G. M. SHELX-76, Program for Crystal Structure Determination; Cambridge, 1976.
(29) Keller, E. SCHAKAL-88. A Fortran Program for the Graphic Representation of Molecular and Crystallographic Models, Freiburg, 1988.
(30) Johnson, C. K. ORTEP II. Report ORNL-5138; Oak Ridge National Laboratory: Oak Ridge, TN, 1971.

Table I. Summary of the Crystal Structure Data

	4a	4c(I)	4c(II)
formula	$C_{15}H_9F_3Fe_3NO_{10}P$	$C_{15}H_9F_3Fe_3NO_{13}P$	$C_{15}H_9F_3Fe_3NO_{13}P$
fw	618.74	666.74	666.74
cryst size, mm	0.2 × 0.3 × 0.2	0.2 × 0.4 × 0.3	0.48 × 0.1 × 0.02
crystallizn solvent	*n*-pentane	*n*-pentane	*n*-pentane
cryst syst	orthorhombic	orthorhombic	triclinic
space group	*Pbca*	*Pbca*	$P\bar{1}$
Z	8	8	2
a, Å	15.294 (12)	15.520 (4)	8.400 (3)
b, Å	15.852 (9)	16.199 (5)	11.735 (5)
c, Å	18.877 (12)	19.626 (4)	13.374 (6)
α, deg	90	90	69.42 (3)
β, deg	90	90	90.37 (3)
γ, deg	90	90	75.65 (3)
V, Å^3	4577	4934	1189
d_{calc}, g cm^{-3}	1.80	1.79	1.86
Mo Kα, Å	0.71069	0.71069	0.71069
abs cor	empirical DIFABS[a]	empirical DIFABS[a]	empirical DIFABS[a]
μ, cm^{-1}	20.4	18.9	19.59
2θ range, deg	4–40	4–40	4–40
hkl range	$0 \le h \le 14, 0 \le k \le 15, 0 \le l \le 18$	$0 \le h \le 14, 0 \le k \le 15, 0 \le l \le 18$	$0 \le h \le 8, -11 \le k \le 11, -12 \le l \le 12$
no. of measd rflns	2446	2629	2420
no. of unique rflns	2136	2308	2220
no. of obsd rflns	1094 $F_o > 3\sigma(F_o)$	1862 $F_o > 2\sigma(F_o)$	1446 $F_o > 3\sigma(F_o)$
no. of variables	148	319	159
temp factors	Fe, P aniso, C, N, F, O iso	Fe, P, C, N, F, O aniso	Fe, P aniso, C, N, F, O iso
w	$[\sigma(F_o)^2 + 0.0015F^2]^{-1}$	1	1
R	11.3	5.6	9.0
R_w	10.6	5.6	9.0
max shift/error	0.001	0.006	0.001
res electr dens	1.46	0.73	1.76

[a] See ref 26.

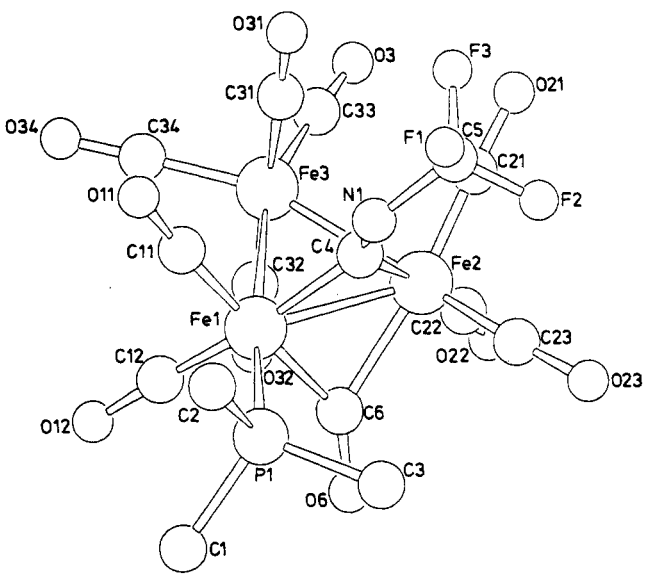

Figure 1. SCHAKAL plot of **4a**.

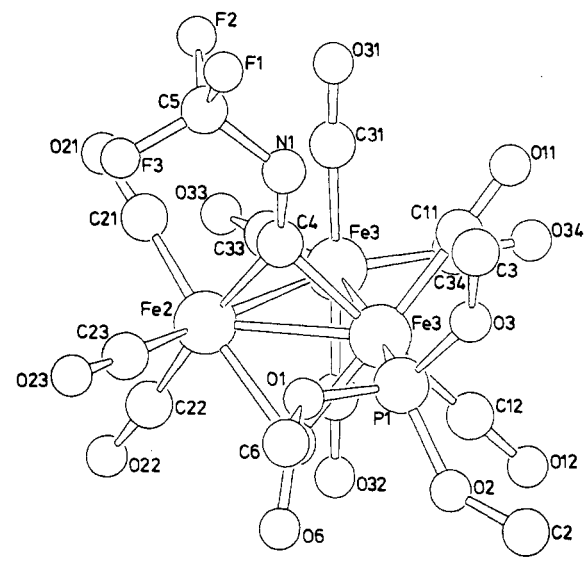

Figure 2. SCHAKAL plot of **4(I)c**.

lengths and angles are summarized in Table VI. The molecular structures and atom numbering schemes are depicted in Figures 1–3.

Results and Discussion

Syntheses. Thermal as well as photolytic substitution reactions of $Fe_3(CO)_{12}$ often proceed only in very low yield.[24] $Fe_3(CO)_{11}(CNCF_3)$ is even less reactive. In early attempts to synthesize phosphite-substituted derivatives starting with $Fe_3(CO)_{11}(CNCF_3)$, only traces of a compound $Fe_3(CO)_{10}(CNCF_3)P(OC_2H_5)_3$ could be isolated.[31] In 1988 Cardin et al.[23] reported a very efficient synthesis for mono- and disubstituted derivatives of $Fe_3(CO)_{12}$ using trimethylamine *N*-oxide in dichloromethane/acetonitrile to

Scheme I

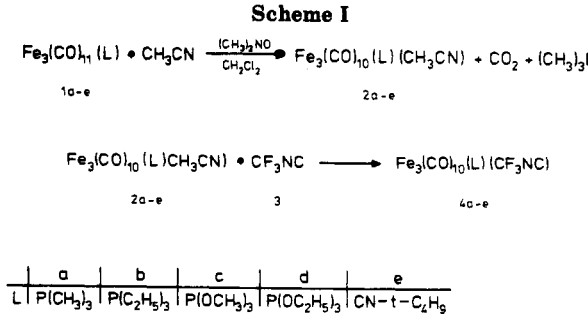

(31) Lentz, D. Unpublished results.

Table II. Fractional Coordinates for $Fe_3(CO)_{10}(\mu\text{-}CNCF_3)[P(CH_3)_3]$, 4a

atom	x	y	z	B_{eq}, Å^2
Fe1	0.1298 (2)	0.8247 (4)	0.1027 (2)	3.21
Fe2	0.1038 (3)	0.6715 (4)	0.0746 (2)	3.60
Fe3	0.2221 (3)	0.7542 (4)	−0.0029 (3)	4.82
P1	0.0550 (6)	0.8698 (7)	0.1971 (5)	4.64
C1	−0.0126 (25)	0.9659 (29)	0.1819 (21)	8.19
C2	0.1263 (19)	0.9044 (25)	0.2702 (16)	5.44
C3	−0.0200 (21)	0.7935 (25)	0.2377 (19)	6.34
C4	0.1625 (16)	0.7238 (19)	0.1510 (15)	2.91
C5	0.2248 (13)	0.6310 (12)	0.2430 (11)	11.48
C6	0.0252 (19)	0.7776 (21)	0.0682 (15)	3.88
C11	0.2254 (20)	0.8641 (23)	0.1312 (16)	4.37
C12	0.1115 (22)	0.9101 (29)	0.0504 (19)	5.63
C21	0.1768 (23)	0.5921 (29)	0.0695 (19)	5.73
C22	0.0526 (24)	0.6349 (28)	0.0018 (22)	7.00
C23	0.0310 (22)	0.6212 (27)	0.1311 (18)	5.95
C31	0.3048 (19)	0.7236 (23)	0.0609 (17)	4.41
C32	0.1378 (23)	0.7876 (27)	−0.0525 (20)	6.74
C33	0.2575 (24)	0.6813 (31)	−0.0631 (21)	7.19
C34	0.2865 (21)	0.8406 (26)	−0.0330 (17)	4.60
F1	0.2492 (13)	0.6452 (12)	0.3093 (11)	15.65
F2	0.1602 (13)	0.5754 (12)	0.2431 (11)	15.96
F3	0.2919 (13)	0.5988 (12)	0.2078 (11)	13.45
N1	0.1966 (14)	0.7109 (18)	0.2126 (14)	4.60
O6	−0.0476 (12)	0.7929 (15)	0.0496 (11)	4.86
O11	0.2895 (16)	0.8861 (18)	0.1605 (13)	7.60
O12	0.0948 (17)	0.9729 (21)	0.0187 (14)	8.37
O21	0.2253 (18)	0.5329 (21)	0.0601 (15)	9.44
O22	0.0100 (17)	0.6150 (18)	−0.0516 (14)	8.12
O23	−0.0200 (16)	0.5816 (19)	0.1688 (14)	8.22
O31	0.3607 (14)	0.7037 (17)	0.0967 (12)	6.62
O32	0.0765 (14)	0.8049 (16)	−0.0924 (12)	6.05
O33	0.2779 (17)	0.6293 (21)	−0.1021 (14)	8.58
O34	0.3278 (16)	0.8983 (19)	−0.0499 (12)	6.63

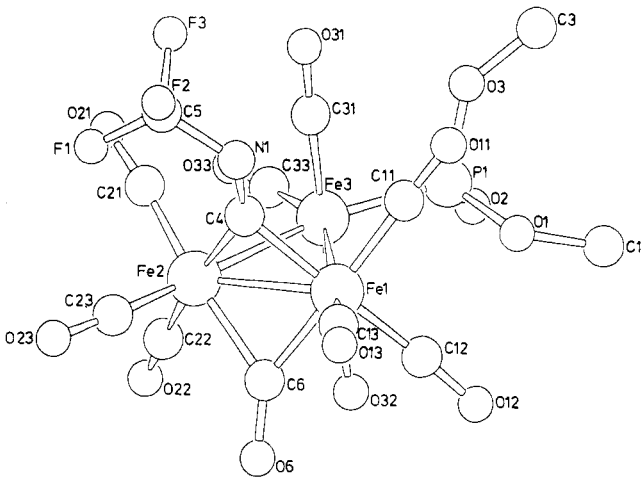

Figure 3. SCHAKAL plot of **4(II)c**.

generate a labile, very reactive acetonitrile complex $Fe_3(CO)_{10}(L)(CH_3CN)$ [L = CO, PR_3, $P(OR)_3$]. Using their method we were able to synthesize the desired cluster compounds in a straightforward reaction (Scheme I). Treatment of $Fe_3(CO)_{11}(L)$ **1** [L = $P(CH_3)_3$ (**a**), $P(C_2H_5)_3$ (**b**), $P(OCH_3)_3$ (**c**), $P(OC_2H_5)$ (**d**), CN-*t*-C_4H_9 (**e**)] with trimethylamine *N*-oxide results in the formation of the acetonitrile complex **2**,[23] which in contrast to $Fe_3(CO)_{11}(RCN)$ (R = CH_3, C_6H_4-2-Me)[23] has not been isolated or further characterized. **2** easily undergoes ligand substitution with trifluoromethyl isocyanide to form the disubstituted cluster compounds **4**.

The infrared spectra (Table V) of all of these compounds **4a–e** exhibit absorptions due to a bridging trifluoromethyl isocyanide and a bridging carbonyl ligand in addition to absorptions which correspond to terminal carbonyl ligands and the terminal *tert*-butyl isocyanide ligand, respectively.

Table III. Fractional Coordinates for $Fe_3(CO)_{10}(\mu\text{-}CNCF_3)[P(OCH_3)_3]$, 4(I)c

atom	x	y	z	B_{eq}, Å^2
Fe1	0.1421 (1)	0.1736 (1)	0.0931 (1)	4.25
Fe2	0.1188 (1)	0.3250 (1)	0.0728 (1)	5.31
Fe3	0.2340 (1)	0.2462 (1)	−0.0058 (1)	5.15
P1	0.0668 (2)	0.1273 (2)	0.1781 (2)	6.26
C1	−0.0498 (10)	0.1911 (13)	0.2637 (9)	12.85
C2	−0.0286 (18)	−0.0107 (13)	0.1665 (12)	19.82
C3	0.1559 (15)	0.0824 (14)	0.2876 (9)	14.35
C4	0.1769 (7)	0.2709 (6)	0.1468 (6)	4.68
C5	0.2366 (6)	0.3514 (4)	0.2364 (4)	8.12
C6	0.0389 (8)	0.2222 (7)	0.0615 (5)	4.91
C11	0.2403 (8)	0.1309 (7)	0.1223 (6)	5.33
C12	0.1183 (8)	0.0900 (8)	0.0370 (6)	5.73
C21	0.1982 (11)	0.4036 (9)	0.0705 (8)	7.99
C22	0.0629 (10)	0.3630 (9)	0.0000 (8)	7.96
C23	0.0445 (10)	0.3705 (10)	0.1309 (8)	7.93
C31	0.3152 (8)	0.2701 (8)	0.0569 (6)	5.69
C32	0.1429 (8)	0.2228 (9)	−0.0575 (6)	6.53
C33	0.2714 (8)	0.3227 (10)	−0.0628 (7)	7.29
C34	0.2917 (9)	0.1599 (10)	−0.0369 (7)	6.89
F1	0.2459 (6)	0.3327 (4)	0.3016 (4)	18.25
F2	0.3103 (6)	0.3815 (4)	0.2133 (4)	18.06
F3	0.1763 (6)	0.4088 (4)	0.2305 (4)	16.90
N1	0.2170 (6)	0.2765 (6)	0.2036 (5)	5.70
O1	0.0153 (6)	0.1971 (6)	0.2140 (5)	8.94
O2	−0.0050 (7)	0.0633 (7)	0.1574 (6)	11.72
O3	0.1150 (9)	0.0775 (9)	0.2357 (6)	13.55
O6	−0.0318 (5)	0.2138 (6)	0.0423 (4)	7.33
O11	0.3040 (6)	0.1047 (6)	0.1430 (5)	7.98
O12	0.1029 (6)	0.0371 (6)	0.0012 (5)	8.49
O21	0.2462 (9)	0.4555 (7)	0.0674 (7)	12.02
O22	0.0264 (8)	0.3918 (8)	−0.0456 (6)	11.52
O23	−0.0020 (8)	0.4020 (8)	0.1685 (6)	11.86
O31	0.3722 (6)	0.2854 (6)	0.0922 (4)	7.87
O32	0.0873 (6)	0.2083 (7)	−0.0948 (5)	8.32
O33	0.2938 (6)	0.3725 (8)	−0.1002 (5)	10.28
O34	0.3299 (7)	0.1046 (7)	−0.0568 (6)	9.94

The ^1H, ^{31}P, and ^{19}F NMR spectra of the phosphine derivatives **4a** and **4b** consist of a single signal. These signals do not show any significant change on varying the recording temperature. In the ^{19}F NMR spectra the resonance of **4a** and **4b** is split into a doublet due to coupling with the phosphorus nucleus. Consequently the phosphorus resonance exhibits a quartet. From these findings we can conclude that **4a** and **4b** exist as single isomers and that the phosphine ligand occupy a position at a bridged iron atom.

The ^1H, ^{19}F, and ^{31}P NMR spectra of the phosphite-substituted clusters, however, exhibit two sets of signals revealing the presence of two isomers in approximate ratio of 1:1. The isomers **4(I)c** and **4(I)d** possess similar coupling constants as **4a** and **4b**, suggesting that these compounds have similar structures. **4(II)c** and **4(II)d** exhibit no significant coupling between the phosphorus and the fluorine atom. For these reasons one can assume that the phosphite ligand in **4(II)c** and **4(II)d** occupies a position at the unbridged iron atom.

According to the ^1H and ^{19}F NMR spectra the *tert*-butyl isocyanide substituted compound **4e** exists as a mixture of at least three isomers. The infrared spectrum exhibits no absorptions for a bridging *tert*-butyl isocyanide ligand. The structure of $Fe_3(CO)_{11}(CN\text{-}t\text{-}C_4H_9)$-*t*) has been established by an X-ray structure determination.[25] In this compound the *tert*-butyl isocyanide ligand occupies the axial position at the unbridged iron atom. In $Fe_3(CO)_{10}(CN\text{-}t\text{-}C_4H_9)_2$ the *tert*-butyl isocyanide ligands are coordinated at an axial and equatorial position of the unbridged iron atom.[32] In solution the molecule is highly

(32) Murray, J. B.; Nicholson, B. K., Whitton, A. J. *J. Organomet. Chem.* **1990**, *385*, 91.

Table IV. Fractional Coordinates for $Fe_3(CO)_{10}(\mu\text{-}CNCF_3)[P(OCH_3)_3]$, 4(II)c

atom	x	y	z	B_{eq}, Å^2
Fe1	0.0393 (4)	0.2188 (3)	0.1822 (2)	3.08
Fe2	0.3026 (4)	0.2884 (3)	0.1706 (3)	3.22
Fe3	0.3322 (4)	0.0397 (3)	0.2393 (3)	3.24
P1	0.2813 (9)	−0.1442 (6)	0.2861 (6)	4.30
C1	0.0410 (36)	−0.2344 (28)	0.2278 (24)	7.26
C2	0.5433 (49)	−0.3034 (35)	0.2513 (30)	10.00
C3	0.2518 (53)	−0.3161 (42)	0.4866 (36)	12.44
C4	0.1439 (27)	0.2866 (21)	0.2712 (18)	4.09
C5	0.1775 (20)	0.3714 (15)	0.4060 (13)	9.23
C6	0.1270 (26)	0.3104 (20)	0.0585 (18)	3.81
C11	−0.0136 (28)	0.1150 (22)	0.3046 (20)	4.34
C12	−0.0371 (27)	0.1455 (21)	0.1033 (18)	4.11
C13	−0.1405 (29)	0.3380 (22)	0.1626 (18)	4.18
C21	0.4636 (31)	0.2436 (23)	0.2722 (20)	4.90
C22	0.4501 (31)	0.2651 (23)	0.0737 (21)	5.23
C23	0.2756 (26)	0.4508 (21)	0.1307 (17)	3.68
C31	0.3242 (27)	0.0351 (21)	0.3753 (19)	4.11
C32	0.3138 (28)	0.0538 (21)	0.1002 (20)	4.42
C33	0.5453 (32)	−0.0123 (24)	0.2531 (20)	5.27
F1	0.2775 (20)	0.4363 (15)	0.3513 (13)	9.88
F2	0.0582 (20)	0.4486 (15)	0.4338 (13)	16.30
F3	0.2626 (20)	0.2818 (15)	0.4942 (13)	16.97
N1	0.0941 (24)	0.3151 (18)	0.3511 (16)	5.20
O1	0.1050 (21)	−0.1340 (16)	0.2403 (14)	5.81
O2	0.3848 (32)	−0.2428 (23)	0.2403 (20)	10.39
O3	0.3022 (31)	−0.2171 (25)	0.4113 (22)	10.90
O6	0.1039 (19)	0.3585 (15)	−0.0389 (13)	5.34
O11	−0.0540 (20)	0.0516 (15)	0.3798 (14)	5.49
O12	−0.0902 (22)	0.1042 (16)	0.0464 (15)	6.38
O13	−0.2634 (22)	0.4181 (17)	0.1532 (14)	6.39
O21	0.5751 (23)	0.2189 (17)	0.3322 (15)	6.67
O22	0.5346 (24)	0.2533 (18)	0.0123 (16)	2.87
O23	0.2677 (20)	0.5605 (17)	0.1047 (14)	5.97
O31	0.3249 (21)	0.0254 (16)	0.4635 (15)	5.97
O32	0.3070 (20)	0.0572 (15)	0.0149 (14)	5.77
O33	0.6899 (26)	−0.0439 (19)	0.2638 (16)	7.91

fluxional, giving rise to only one signal in the ^{1}H NMR spectrum.[32]

Crystal Structure Determination. Since ^{13}C NMR studies carried out in order to facilitate the assignment of the carbonyl resonances would be worthless without the knowledge of the solid-state structures, we determined the structure of compound **4a** and both isomeric forms of **4c**. The crystallographic data of the compounds **4a**, **4(I)c**, and **4(II)c** are summarized in Table I; the atomic coordinates and temperature factors are listed in Tables II–IV. The molecular structure and atomic numbering scheme are depicted in Figures 1–3. Important bond lengths, contact distances, and angles are summarized in Table VI.

The crystals of these compounds are built up by discrete molecules which show no unusual intermolecular distances. The isostructural compounds **4a** and **4(I)c** both are orthorhombic, space group *Pbca* with very similar lattice constants (Table I). All of these molecules contain a nearly isosceles triangle of iron atoms. As expected, the Fe–Fe distances of the bridged metal atoms are significantly shorter than the unbridged Fe–Fe bonds. The same tendency has been observed in all derivatives of $Fe_3(CO)_{12}$ of known structure, $Fe_3(CO)_{12}$,[1,14] $Fe_3(CO)_{11}[P(C_6H_5)_3]$,[33] $Fe_3(CO)_{11}(CN\text{-}t\text{-}C_4H_9)$,[25] $Fe_3(CO)_{11}(CNCF_3)$,[19] $Fe_3(CO)_{10}[P(OCH_3)_3]_2$,[18] and $Fe_3(CO)_9[P(CH_3)_2(C_6H_5)]_3$.[34] For the compounds **4a** and **4(I)c** the Fe–Fe distances of the unbridged iron–iron bonds are equal within the standard deviations. In **4(II)c**, however, the distance Fe(1)–Fe(3) [2.709 (4) Å] is significantly longer than Fe(2)–Fe(3) [2.679 (4) Å]. In all of these compounds both bridging positions are occupied by the trifluoromethyl isocyanide and one carbonyl ligand, respectively. Both bridges show a striking asymmetry. The bond Fe(2)–C(4) and the quasi opposite bond Fe(1)–C(6) are short, whereas Fe(2)–C(6) and Fe(1)–C(4) are long. In all these three compounds the asymmetry of the carbonyl bridge is much more distinct than the asymmetry of the trifluoromethyl isocyanide bridge. In contrast, both bridges in $Fe_3(CO)_{11}(CNCF_3)$ are nearly symmetrical,[19] whereas in $Fe_3(CO)_{12}$, which contains two carbonyl bridges, this asymmetry is more distinct. The compounds $Fe_3(CO)_{11}[P(C_6H_5)_3]$,[33] $Fe_3(CO)_{10}[P(OCH_3)_3]_2$,[18] and $Fe_3(CO)_9[P(CH_3)_2(C_6H_5)]_3$[34] also possess asymmetric bridges, too.

The position of the phosphorus ligand in these compounds is of particular interest. The compounds **4a** and **4(I)c** are isostructural. In both compounds the phosphine and phosphite ligands occupy the equatorial position within the planes of the iron atoms at the bridge iron atom Fe1, respectively. In contrast, the phosphite ligand in **4(II)c** is coordinated to the unbridged iron atom Fe3. In respect to the phosphorus ligands the same isomers have been observed in the crystal structure determination of $Fe_3(CO)_{11}[P(C_6H_5)_3]$,[33] which contains two independent molecules in the unit cell. As in the case of all phospho-

Table V. Spectroscopic Data for the Compounds 4a–e

	IR[a]	^{1}H NMR[b]	^{19}F NMR[b]	^{31}P NMR[b]
4a	2089 (m)	1.49	−57.1	19.0
	2037 (vs)	$^2J_{PH}$ = 10 Hz	$^5J_{PF}$ = 2.7 Hz	
	2018 (vs)			
	2012 (sh)			
	1994 (m)			
	1986 (w)			
	1855 (w)			
	1641 (w)			
4b	2087 (s)	1.19 (CH_3)	−56.8	38.4
	2035 (vs)	$^3J_{HH}$ = 7.6 Hz	$^5J_{PF}$ = 2 Hz	
	2015 (vs)	$^3J_{PH}$ = 15 Hz		
	1998 (sh)	1.92 (CH_2)		
	1983 (sh)	$^2J_{PH}$ = 7.8 Hz		
	1861 (w)			
	1635 (w)			
4c	2091 (m)	3.80	−56.9 (I)	150.1 (I)
(I/II)	2043 (vs)	$^3J_{PH}$ = 11 Hz	J_{PF} = 3, 1 Hz (I)	
	2022 (vs)		−56.7 (II)	159.4 (II)
	1895 (vw)			
	1861 (w)			
	1664 (w)			
4d (I/II) +10 °C	2090 (m)	1.39/1.42	−56.9 (I)	145.5 (I)
	2041 (vs)	J_{PH} = 7/7 Hz	J_{PF} = 2.9 Hz (I)	
	2021 (vs)	4.18/4.15	−56.7 (II)	155.1 (II)
	1989 (w)			
	1862 (w)			
	1657 (w)			
4e	2174 (w)	1.5	−56.7 (I)	
(I/II/III)				
	2085 (w)	1.7	−56.5 (II)	
	2047 (vs)		−55.6 (III)	
	2037 (vs)			
	2019 (s)			
	2004 (m)			
	1989 (w)			
	1870 (vw)			
	1844 (vw)			
	1664 (w)			

[a] Solutions in *n*-hexane (**4a**,**c**,**d**,**e**) and dichloromethane (**4b**). [b] Solutions in $CDCl_3$.

(33) Dahn, D. J.; Jacobson, R. A. *J. Chem. Soc., Chem. Comm.* **1966**, 496; *J. Am. Chem. Soc.* **1968**, *90*, 5106.
(34) McDonald, W. S.; Moss, J. R.; Raper, G.; Shaw, B. L.; Greatrex, R.; Greenwood, N. N. *J. Chem. Soc., Chem. Comm.* **1969**, 1295. Raper, G.; McDonald, W. S. *J. Chem. Soc. A* **1971**, 3430.

Table VI. Important Bond Lengths (Å) and Angles (deg) for 4a, 4(I)c, and 4(II)c

	4a	4(I)c	4(II)c
	Bond Lengths		
Fe(1)–Fe(2)	2.518 (7)	2.512 (2)	2.529 (4)
Fe(2)–Fe(3)	2.672 (7)	2.685 (2)	2.679 (4)
Fe(1)–Fe(3)	2.687 (7)	2.682 (2)	2.709 (4)
Fe(1)–P(1)	2.23 (1)	2.172 (3)	
Fe(3)–P(1)			2.178 (7)
Fe(1)–C(4)	1.91 (3)	1.97 (1)	1.96 (2)
Fe(2)–C(4)	1.89 (3)	1.92 (1)	1.90 (2)
Fe(1)–C(6)	1.88 (3)	1.89 (1)	1.90 (2)
Fe(2)–C(6)	2.07 (3)	2.09 (1)	2.00 (2)
C(4)–N(1)	1.29 (3)	1.28 (1)	1.27 (3)
C(6)–O(6)	1.19 (3)	1.17 (1)	1.22 (2)
$Fe–CO_{term}$	1.68 (3)–1.81 (3)	1.77 (2)–1.80 (2)	1.73 (2)–1.84 (3)
	Bond Angles		
Fe(1)–Fe(2)–Fe(3)	62.3 (2)	62.0 (1)	62.6 (1)
Fe(2)–Fe(1)–Fe(3)	61.7 (2)	62.2 (1)	61.4 (1)
Fe(1)–Fe(3)–Fe(2)	56.1 (2)	55.8 (1)	56.0 (1)
Fe(1)–C(4)–Fe(2)	83 (1)	80.4 (5)	82.0 (9)
Fe(1)–C(6)–Fe(2)	79 (1)	78.1 (4)	80.9 (9)

Table VII. Signal Assignment of the ^{13}C NMR Resonances for the Compounds 4a, 4b, and $Fe_3(CO)_{11}(CNCF_3)$

4a			4b			$Fe_3(CO)_{11}(CNCF_3)$	
	δ, ppm	^2J(PC), Hz		δ, ppm	^2J(PC), Hz		δ, ppm
Ch	279.3		Ch	279.1		Ch	271.5 (^3J(CF) = 7 Hz)
Cg	235.2	13.4	Cg	233.5	12.0	Cg	236.4
Cf	219.5		Cf	218.8		Cf	217.1
Ce	216.6		Ce	216.0		Ce	215.3
Ca′	213.9	15.9	Ca′	214.8	15.0	Ca′	210.4[a]
Cc′	210.5	14.6	Cc′	210.8	16.0	Cc′	208.2[a]
Ca	210.6		Ca	211.0		Ca	209.2[a]
Cc	209.3		Cc	209.3		Cc	207.9[a]
Cd	205.1		Cd	204.9		Cd	204.3
Cd′	204.7		Cd′	204.7		Cd′	204.3
Cb	202.8		Cb	202.8		Cb	200.4[b]
						Cb′	199.8[b]

[a,b] The signals marked with *a* or *b* may be interchanged.

Scheme II

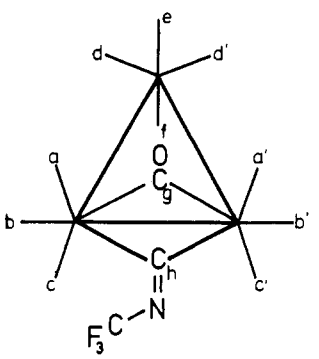

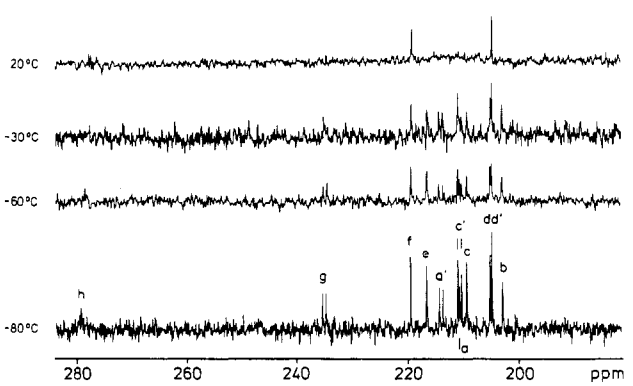

Figure 4. Variable-temperature ^{13}C NMR spectra of **4a**.

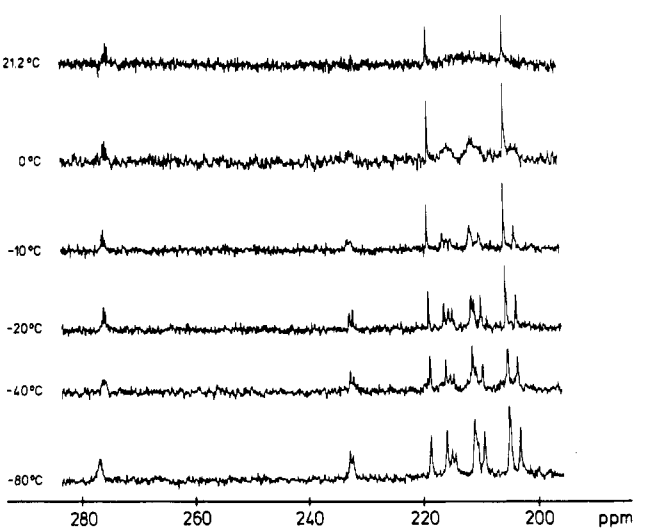

Figure 5. Variable-temperature ^{13}C NMR spectra of **4b**.

rus-substituted derivatives[18,33,34] of $Fe_3(CO)_{12}$, the phosphorus ligands lie within the plane of the iron atoms, the so-called equatorial position. In addition, the ruthenium and osmium derivatives $M_3(CO)_{12-n}L_n$ (M = Ru, Os; $1 < n < 4$; L = phosphine and phosphite) contain the ligand L within the plane of the metal triangle.[35]

^{13}C NMR Spectroscopic Studies. According to the ^{13}C NMR spectra, the compounds **4a–d** are nonrigid at ambient temperature. **4a–d** possess a high solubility in

(35) Bruce, M. I.; Liddbell, M. J.; Hughes, C. A.; Patrick, J. M.; Skelton, W.; White, A. H. *J. Organomet. Chem.* **1988**, *347*, 181. *J. Organomet. Chem.* **1989**, *369*, 3430.

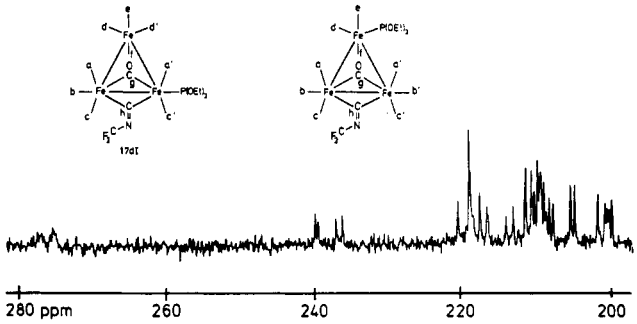

Figure 6. ^{13}C NMR spectra of **4(I/II)d** at −80 °C. Peaks are as follows: 276.0, 273.3 (Ch), 239.5 ($^2J_{CF}$ = 10.7 Hz), 236.5 ($^2J_{CF}$ = 18.9 Hz) (Cg), 216–221 (Ce,f), 207–214 (Ca,a′,c,c′), 199–206 (Cb,b′,d,d′).

sulfuryl chloride fluoride even at −80 °C, which is scarcely influenced by the addition of about 10% dideuteriodichloromethane. This allows low-temperature ^{13}C NMR spectroscopic measurements with natural abundant ^{13}C content even at −80 °C.

The Phosphine Derivatives 4a and 4b. The two phosphine-substituted compounds **4a** and **4b** (phosphine ligand in position b′, Scheme II) exhibit at −80 °C all of the 11 resonances expected between 200 and 300 ppm (Figures 4 and 5, Table VII). The signals at 279.3 and 279.1 ppm, respectively, appear as hardly resolved multiplets, due to coupling with the phosphorus and fluorine nuclei, respectively. They can be easily assigned to the isocyanide carbon atom C(h) (Scheme II) in accordance with a chemical shift of 271.5 ($^3J_{CF}$ = 7.5 Hz) observed for $Fe_3(CO)_{11}(CNCF_3)$.[19,20] In contrast to $Fe_3(CO)_{11}(CNCF_3)$,[20] the assignment of the resonance of the bridging carbonyl group C(g) can be made without ambiguity, due to coupling with the phosphorus nucleus of the phosphine ligand. They are observed low field with respect to all other carbonyl carbon atom resonances at 235.2 and 233.5 ppm, respectively. For $Fe_3(CO)_{11}(CNCF_3)$ the signal at 204.3 ppm, which possesses double intensity, has been assigned to the nearly equivalent equatorial carbonyl carbon atom C(d) and C(d′). These carbonyl groups differ only in the their relative position to the CF_3 group of the isocyanide ligand.[20] In accordance with this assignment the resonances at 205.1, 204.7 (**4a**) and 204.9, 204.7 (**4b**), respectively, are due to the equatorial carbonyl carbon atoms of the $Fe(CO)_4$ moiety of **4a** and **4b**. Due to the phosphorus substitution, these positions become nonequivalent. The signals at 213.9 ($^2J_{PC}$ = 15.9 Hz), 210.5 ($^2J_{PC}$ = 14.6 Hz) (**4a**) and 214.8 ($^2J_{PC}$ = 15.0 Hz), 210.8 ($^2J_{PC}$ = 16.0 Hz) (**4b**), respectively, are split into doublets as a result of coupling with the phosphorus atom of the ligand. They can assigned to the axial position C(a′) and C(c′) of the Fe(L)$(CO)_2$ moiety. There remain two further resonances in this chemical shift area at 210.6, 209.3 (**4a**) and 211.0, 209.3 ppm (**4b**), respectively, which now can logically assigned to the axial carbonyl carbon atoms of the $Fe(CO)_3$ group. An unambigious assignment of the two remaining low-field signals at 219.5, 216.6 (**4a**) and 218.8, 216.0 ppm (**4b**) arise from the expectation that the two axial carbonyl carbon atoms of the $Fe(CO)_4$ moiety should have similar chemical shifts as the axial carbonyl atoms of the $Fe(CO)_3$ moiety. For that reason these signals belong to the carbon atoms C(e) and C(f). The single high-field signal at 202.8 ppm can now be assigned to the equatorial position of the Fe$(CO)_3$ group C(b). Consequently, $Fe_3(CO)_{11}(CNCF_3)$[20] shows two high-field signals, as there are two different $Fe(CO)_3$ units. There is no way to distinguish experimentally between the resonances of carbonyl carbon atoms

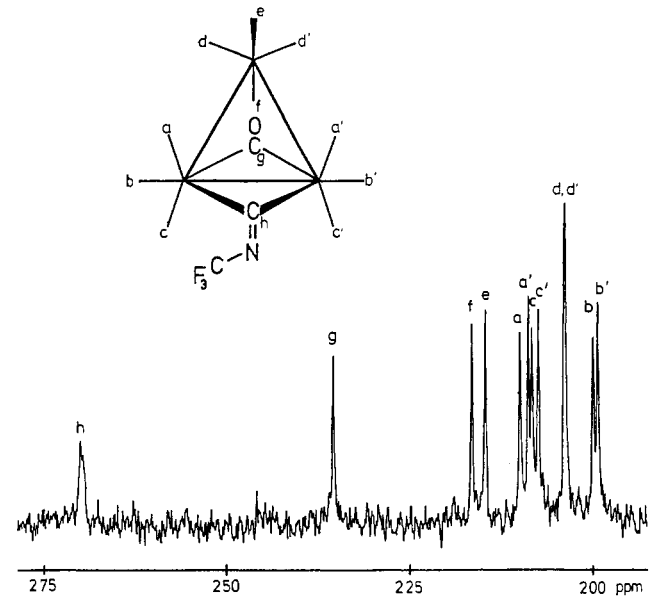

Figure 7. ^{13}C NMR spectra of $Fe_3(CO)_{11}(\mu_3\text{-}CNCF_3)$ at −100 °C.

below or above the plane of iron atoms.

The Phosphite Derivatives 4c and 4d. The two phosphite-substituted compounds **4c** and **4d** consist of a mixture of two isomers. As expected their ^{13}C NMR spectra (Figure 6) are much more complicated, and therefore, a complete assignment of all resonances is impossible. Nevertheless a partial assignment of the ^{13}C NMR spectrum of **4d** can be made with the aid of the knowledge of the spectra of **4a** and **4b**.

As expected, the signals of the bridging trifluoromethyl isocyanide carbon atoms are observed as poorly resolved multiplets at 276.0 and 274.3 ppm. The two doublets at 239.5 and 236.5 ppm belong to the bridging carbonyl carbon atoms C(g). The small ^{13}C–^{31}P coupling constant of 10.7 Hz of the signal at 239.5 ppm allows the assignment of this resonance to the isomer **4(II)d**. Consequently, the signal a with large coupling constant of 18.9 Hz is due to isomer **4(I)d**. In comparison with spectra of the compounds **4a,b** and $Fe_3(CO)_{11}(CNCF_3)$, the high-field signals at 201.7, 200.7, and 199.8 ppm can be assigned to the equatorial positions of the $Fe(CO)_3$ moiety. The signals at 205.3 and 204.8 ppm are due to the equatorial carbonyl carbon atoms of the $Fe(CO)_4$ group of **4(I)d**. Because of the ^{13}C–^{31}P coupling constant of 17.4 Hz the resonance at 200.3 ppm results from the single equatorial carbonyl carbon atom C(d) of the isomer **4(II)d**. The group of signals between 216–221 ppm and 207–214 ppm can be assigned to the axial carbon atoms of the $Fe(CO)_4$ and $Fe(CO)_3$ groups, respectively. A more detailed assignment, however, does not seem to be possible for these resonances.

Undecacarbonyl(μ-trifluoromethyl isocyanide)triiron. The ^{13}C NMR spectrum[20] of $Fe_3(CO)_{11}(CNCF_3)$ at −100 °C (Figure 7, Table VII) exhibits 11 of the 12 signals expected from the solid-state structure[19] between 190 and 300 ppm.

Only two of these signals could be assigned unambiguously thus far.[20] The resonance at 204.3 ppm possesses double intensity and can be assigned to the closely equivalent carbonyl carbon atoms C(d) and C(d′). Due to the ^{13}C–^{19}F coupling of about 7–8 Hz the lowest field signal is consistent only with the trifluoromethyl isocyanide carbon atom. The previously made assignment[20] and exchange mechanism has been speculative and erroneous.

With the knowledge from the ^{13}C NMR spectra of **4a,b** and **4d** it is possible to assign the ^{13}C NMR spectra of

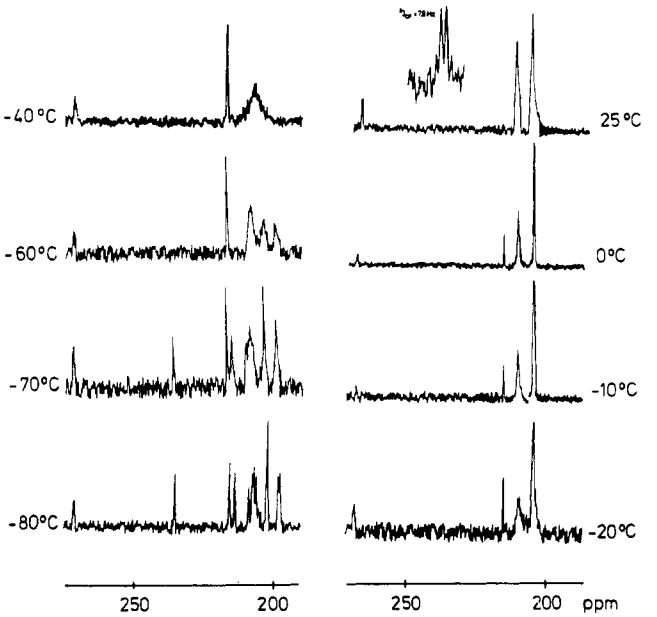

Figure 8. Variable-temperature ^{13}C NMR spectra of $Fe_3(CO)_{11}(\mu_3\text{-}CNCF_3)$.

$Fe_3(CO)_{11}(CNCF_3)$ as follows: The low-field signal at 236.4 ppm is due to the bridging carbonyl carbon atom C(g). The axial carbon atoms C(e) and C(f) of the $Fe(CO)_4$ group exhibit resonances at 215.3 and 217.1 ppm, respectively. The signals at 207.9, 208.7, 209.2, and 210.4 can be assigned to the axial carbon atoms C(a), C(a'), C(c), and C(c') of the $Fe(CO)_3$ moieties. The remaining resonances at 199.8 and 200.4 ppm belong to the equatorial carbon atoms C(b) and C(b').

Variable-Temperature ^{13}C NMR Studies. The variable-temperature ^{13}C NMR spectra of **4a,b** and $Fe_3(CO)_{11}(CNCF_3)$ are represented in Figures 4, 5 and 8. Of the two compounds **4a** and **4b**, **4a** is much less soluble than **4b**. This difference in solubility influences the quality of the spectra. As the signal of the isocyanide carbon atom is split into a multiplet, due to coupling with the phosphorus and fluorine nuclei, this signal can is barely observed for **4a**. The spectra of **4b** were recorded between −80 °C and ambient temperature. Up to −30 °C the resonances of **4a** and **4b** are sharp. The compounds are rigid on the NMR time scale. Above −30 °C a broadening for most of the signals can be observed, resulting in three unchanged sharp signals and one very broad signal at ambient temperature. On warming above +40 °C the formation of new still broad signals at 212 and 208 ppm could be observed. Due to decomposition reactions of $Fe_3(CO)_{10}[P(CH_3)_3](\mu_2\text{-}CNCF_3)$ at higher temperatures forming $Fe_3(CO)_8[P(CH_3)_3](\mu_3\text{-}\eta^2\text{-}CNCF_3)$,[36] the high-temperature limiting spectrum of the fast exchange could not be observed. From these experimental results the following conclusions can be made for the compound **4b**:

(1) Within the observed temperature range two carbonyl ligands do not participate in the exchange process. These are one axial and one equatorial ligand of the $Fe(CO)_4$ moiety.

(2) The isocyanide bridging ligand is not involved in the exchange process.

(3) The bridging carbonyl ligand, however, participates in this fluxional process.

With the above-made reassignment of the low-temperature ^{13}C NMR spectra, the variable-temperature ^{13}C NMR spectra[20] (Figure 8) of $Fe_3(CO)_{11}(CNCF_3)$ can be interpreted. Above −80 °C broadening of most of the resonances occurs leading to the high-temperature limiting spectrum for the exchange process at 0 °C, which consists of two unchanged signals at 217.9 and 269.1 ppm and two new signals at 207.7 and 212.9 ppm. The coalescence temperature is observed at −40 °C. From the experimental results one can conclude as follows:

Up to 0 °C the bridging isocyanide ligand and one axial carbonyl ligand do not participate at the exchange process, whereas all other carbonyl ligands, including the bridging carbonyl group, are permutated in such a way that two signals are observed in the spectrum of fast exchange. In addition rapid, inversion occurs at the nitrogen atom of the isocyanide ligand.

None of the mechanisms provided so far for the exchange process in $Fe_3(CO)_{12}$ fits the experimental spectra of $Fe_3(CO)_{11}(CNCF_3)$ and **4b**. Both the Cotton and Troup "merry-go-round" mechanism[14] and the mechanism of Johnson,[15] which involves the rotation of the iron triangle around its pseudo 2-fold axis, require a simultaneous opening and closing of the two bridges. The complicated icosahedron–cuboctahedron–icosahedron rearrangement mechanism suggested by Johnson et al.[17a] to explain the fluxional behavior of phosphine- and phosphite-substituted derivatives of dodecacarbonyltriiron does not fit the experimental spectra obtained for **4b** and $Fe_3(CO)_{11}(CNCF_3)$.

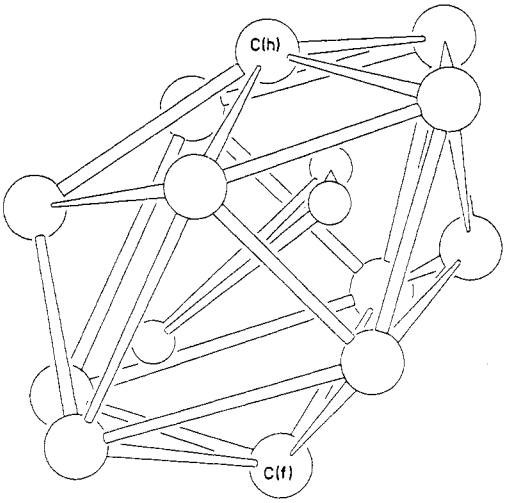

Figure 9. SCHAKAL plot of the ligand polyhedron of $Fe_3(CO)_{11}(\mu_3\text{-}CNCF_3)$.

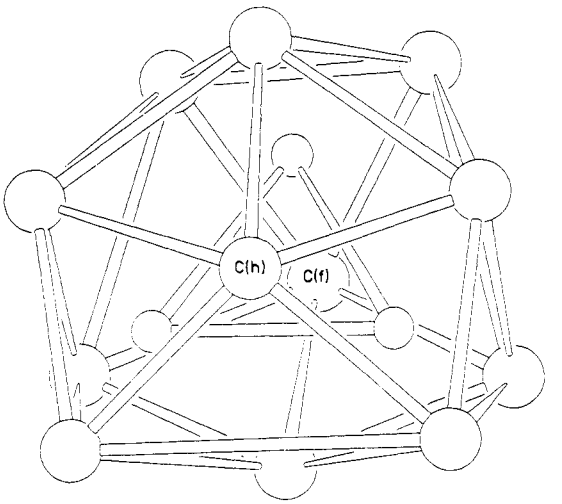

Figure 10. SCHAKAL plot of the ligand polyhedron of $Fe_3(CO)_{11}(\mu_3\text{-}CNCF_3)$, view along the pseudo 5-fold axis.

(36) Lentz, D.; Marschall, R. *Chem. Ber.*, in press.

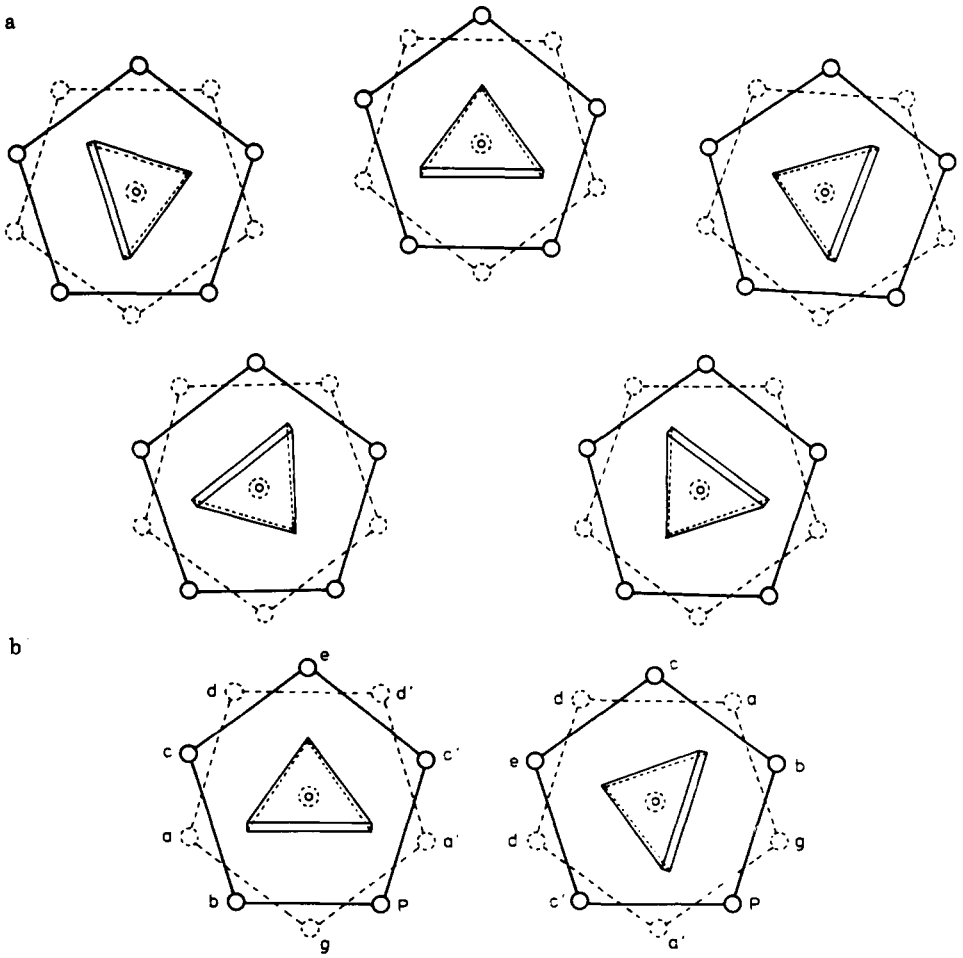

Figure 11. Schematic representation of the rotation of the iron triangle within the ligand polyhedron (a) for $Fe_3(CO)_{11}(\mu\text{-}CNCF_3)$, and (b) for **4a** and **4b**.

The previously proposed mechanism[20] for $Fe_3(CO)_{11}(CNCF_3)$ was based on a wrong assignment of the carbonyl resonances.

Any mechanism has to make allowance for the fact that for $Fe_3(CO)_{11}(CNCF_3)$ there are two ligands, the isocyanide bridge and an axial carbonyl ligand at the $Fe(CO)_4$ moiety, which do not participate in the ligand exchange process.

According to the crystal structure determinations, the ligand atoms of $Fe_3(CO)_{11}(CNCF_3)$ and its phosphine- and phosphite-substituted derivatives **4a,b,(I)c,d** and **4(II)c,d** form a distorted icosahedron (Figure 9). In Figure 9 this ligand icosahedron is oriented in a way that the axial carbonyl ligand C(f) of the $Fe(CO)_4$ group is at the bottom corner and the isocyanide ligand C(h) is at the top corner of the icosahedron. Figure 10 shows a view at the top of the ligand polyhedron along the axis C(f)–C(h). The same orientation is represented in a schematic way in Figure 11a. If we now allow rotation of the ligand polyhedron around its pseudo 5-fold axis through the atoms C(f) and C(h), all carbonyl carbon atoms in the upper and lower pentagon become equivalent, respectively. The carbon atoms C(f) and C(h), which lie on the symmetry element, do not change their environment. This would result in a 5:5:1:1 signal pattern in the 0 °C high-temperature limiting spectrum of $Fe_3(CO)_{11}(CNCF_3)$. The weighted average chemical shifts of the signals are expected to be 206.4 and 212.9 or 207.0 and 212.3, respectively, depending on the assignment of the very similar chemical shifts of the axial carbonyl carbon atoms of the $Fe(CO)_3$ group. These values are in excellent agreement with the experimental values of 207.7 and 212.9 ppm.

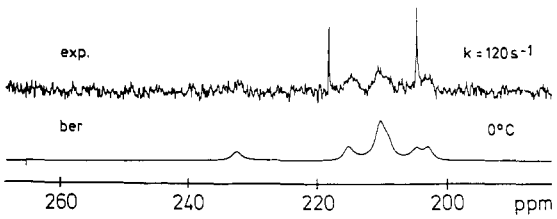

Figure 12. Experimental (0 °C) and simulated ^{13}C NMR spectrum of **4b**.

The situation changes drastically if we have a phosphine ligand attached in the equatorial position C(b′) as observed for the compounds **4a** and **4b**. Rotation of the ligand polyhedron or vice versa the iron triangle by an angle of more than 72° would bring the phosphine ligand into an axial position. In none of the several structure determinations of phosphine or phosphite substituted derivatives of $Fe_3(CO)_{11}$ have the phosphorus ligand been observed in an axial position.[18,33,34] We can conclude that such a position is unfavored for a phosphorus ligand. A 72° rotation of the polyhedron, however, would convert one enantiomer into the other. This results in permutation of the carbonyl carbon atoms C(b) and C(c′), C(a) and C(d′), C(a′) and C(g), C(c) and C(e) (Figure 11b), whereas the carbonyl carbon atoms C(d) and C(f) remain unchanged as does the isocyanide carbon atom. This closely fits the observed spectrum of **4b** at ambient temperature, which consists of three unchanged signals at 277.5, 219.1, and 205.2 and a very broad resonance around 211 ppm. In addition, a line-form analysis[37] with the permutation

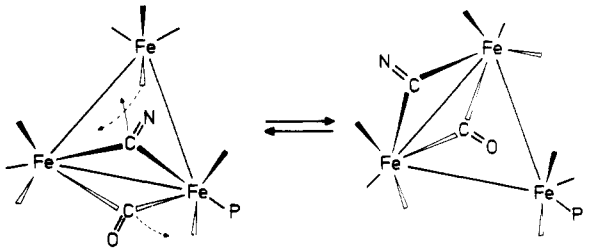

Figure 13. Schematic representation of the isomerization of **4(I)c,d** and **4(II)c,d.**

mentioned above is in good agreement with the experimental spectra (Figure 12). From the coalescence temperature and the line-form analysis the free enthalpies of activation for $Fe_3(CO)_{11}(CNCF_3)$ and **4b** can be estimated as 10 and 13 kcal/mol, respectively.

The Isomerization of the Phosphite-Substituted Derivatives 4c,d. The compounds **4c** and **4d** exist as a mixture of the isomers I and II. These isomers rapidly isomerize on the NMR time scale at elevated temperatures. From variable-temperature ^{19}F and ^1H NMR spectroscopic studies a free enthalpy of activation of 16.5 and 16.3 kcal/mol can be estimated. However, the above discussed ligand exchange mechanism does not rationalize this isomerization, as the phosphite ligand in the two isomers occupy different pentagonal planes in the ligand icosahedron. Also, there exists a higher energy process for $Fe_3(CO)_{11}(CNCF_3)$, which makes all ligands equivalent on the NMR time scale and consequently requires opening of the isocyanide bridge. Since the isomerization of I and II has a higher energy barrier, we now can allow opening and closing of the isocyanide bridge.

(37) DNMR5 (Stephenson, D. S.; Binsch, G. München 1978, Quantum Chemistry Program Exchange, Indiana University, modified by Lehmann, C. Freie Universität Berlin, 1989): Stephenson, D. S.; Binsch, G. *J. Magn. Reson.* **1978**, *32*, 145.

As can be seen from the crystal structure determinations of the different compounds, both bridges are asymmetric. Opening of the longer iron–carbon bonds to the bridging ligands, followed by closing of the isocyanide bridge and the carbonyl bridge along the other iron–iron bond interconverts isomer I into isomer II. The mechanism, schematized in Figure 13, corresponds to the classical "merry-go-round" mechanism proposed by Cotton and Troup for dodecacarbonyltriiron. A rotation of the iron triangle around the pseudo 2-fold axis as it has been proposed by Johnson for $Fe_3(CO)_{12}$ would not interconvert isomer I into isomer II. Therefore, we can assume that the high-energy exchange process for all our compounds is the classical "merry-go-round" mechanism. Due to the high tendency of the trifluoromethyl isocyanide ligand to occupy the bridging position, this mechanism possesses a higher activation energy than the rotation of the ligand polyhedron around its pseudo 5-fold axis, which is the low-energy process.

The rotation of the ligand polyhedron around the pseudo 5-fold axis can explain the equivalence of the carbonyl carbon atoms of $Fe_3(CO)_{12}$ on the NMR time scale as well. However, this fact does not imply that this mechanism is the lowest energy process for $Fe_3(CO)_{12}$. As we have seen from our studies, very small modifications in the ligand sphere can have a drastic influence on the exchange process.

Acknowledgment. This research was supported by the Deutsche Forschungsgemeinschaft and the Fonds der Chemischen Industrie. We acknowledge Prof. Dr. J. Fuchs for his assistance in the crystallographic work.

Supplementary Material Available: Tables listing anisotropic temperature factors, interatomic distances, and interatomic angles for **4a**, **4(I)c**, and **4(II)c** and a figure showing an ORTEP plot of **4(I)c** (10 pages); listings of observed and calculated structure factors (17 pages). Ordering information is given on any current masthead page.